

An Interferometry Imaging Beauty Contest

Peter R. Lawson¹, William D. Cotton², and Christian A. Hummel³
John D. Monnier⁴, Ming Zhao⁴,
John S. Young⁵, Hrobjartur Thorsteinsson⁵,
Serge C. Meimon⁶, Laurent Mugnier⁶, Guy Le Besnerais⁶,
Eric Thiébaud⁷, Peter G. Tuthill⁸

¹Jet Propulsion Laboratory, California Institute of Technology, Pasadena, CA, USA

²National Radio Astronomy Observatory, Charlottesville, VA, USA

³European Southern Observatory, Santiago, Chile

⁴University of Michigan, Ann Arbor, MI, USA

⁵Astrophysics Group, Cavendish Laboratory, Cambridge, United Kingdom

⁶Office National d'Etudes et de Recherches Aérospatiales, Chatillon, France

⁷CRAL / Observatoire de Lyon, Saint Genis Laval, France

⁸School of Physics, University of Sydney, NSW, Australia

ABSTRACT

We present a formal comparison of the performance of algorithms used for synthesis imaging with optical/infrared long-baseline interferometers. Five different algorithms are evaluated based on their performance with simulated test data. Each set of test data is formatted in the OI-FITS format. The data are calibrated power spectra and bispectra measured with an array intended to be typical of existing imaging interferometers. The strengths and limitations of each algorithm are discussed.

Keywords: astronomical software, closure phase, aperture synthesis, imaging, optical, infrared, interferometry

1. INTRODUCTION

Synthesis imaging at optical/infrared wavelengths is a relatively new development. The technique was first proven possible in 1987 with aperture masking experiments.¹ Following that success several new long-baseline interferometers were designed for imaging, and their first images were produced in 1995 and 1996. Very few images have so far been published in the refereed literature. All of these images have relied on radio interferometry software.

One of the longstanding problems in this field is that the available radio astronomy software is unsuited to optical data. Imaging interferometers at optical/infrared wavelengths measure only squared visibilities, bispectra, and their respective errors, with closure phases being calculated from the bispectra. The baseline phases are so corrupted by random atmospheric time-delays at each telescope that the baseline phases are useless, although the closure quantities remain good observables. At radio wavelengths, on the other hand, the visibility amplitudes and phases are the observables; software that processes radio data requests this data as input. It follows that in order to use software packages such as the Astronomical Image Processing System (AIPS) the optical data *must* be transformed: visibilities must be estimated from squared-visibilities, and baseline phases must be derived from closure phases. Although this may work well for bright sources, the assumptions are problematic when dealing with faint sources at low signal-to-noise level. For example, the errors expected from visibility-squared measurements cannot be easily converted to visibility errors. Moreover, optical closure-phase measurements typically have errors of several degrees, whereas radio closure-phase measurements are assumed to have no errors at all. It follows that images derived from optical data, processed through radio interferometry software, may have artifacts and statistics that arise from this process alone.

Further author information: Send correspondence to Peter Lawson, Jet Propulsion Laboratory, MS 301-451, 4800 Oak Grove Drive, Pasadena, CA 91109-8099, USA. E-mail: Peter.R.Lawson@jpl.nasa.gov; Telephone: +1 (818) 354-0747.

Recognizing the above problems, it has been evident for many years that new software is needed that is specifically tailored to optical data. In June 2000, the National Science Foundation hosted a meeting in Socorro, New Mexico, to address issues specific to imaging in optical interferometry.² A first modest step forward, suggested at the meeting, was to establish a common data format for calibrated optical/infrared interferometry data. The Optical Interferometry Exchange Format was released in 2003 and is described elsewhere in these proceedings.³ At the 2001 meeting of the IAU Working Group on Optical/IR Interferometry, David Buscher suggested that the existing software suites should be compared with controlled data sets, and so the subject of an imaging beauty contest was born. Organizing and running the beauty contest was the central activity of the IAU Working Group in 2003–2004.

2. MOTIVATION AND FRAMEWORK OF A BEAUTY CONTEST

There were several motivations for the imaging beauty contest: (1) Encourage the use of the OI Exchange Format, identify problems in its definition, and revise it as necessary; (2) Engage the interferometry community in a formal assessment of existing software; (3) Encourage the development of new software tailored to the needs of optical interferometry.

2.1. Choice of Contest Data

In discussions between the organizers and the participants, there was broad general agreement of the approach and philosophy that should *ideally* be used to guide the contest. Although it proved difficult to follow this ideal, these concerns can be described briefly. The contest data sets should faithfully represent measurements from a plausible long-baseline stellar interferometer. Moreover, the data sets should be relevant to concerns that are particular to optical/infrared long-baseline interferometry, and each set of contest data should test something very specific. The following characteristics were therefore considered:

- The contest data should have about $N(N - 1)/2$ u - v points per hour of observing and fewer bispectrum points, where N is the number of telescopes in the array. This would be consistent with an array of three or four telescopes, reconfigured one or more times.
- The observables must be power spectra and bispectra, which is to say squared-visibilitys and closure quantities.
- The test data should represent a source with a complicated symmetry so that measurements of closure phases are essential for image reconstruction. Parametric imaging (modelling) should not recover all of the source structure in the absence of a priori knowledge. Such an example might be one or more compact sources embedded in an extended asymmetric shell.
- The data might have many, perhaps all, samples in the low signal-to-noise regime.
- The data might include incomplete or sporadic measurements of closure phases and visibilitys, due to telescopes that are sometimes present and other times absent in the data.
- The relationship between u - v coverage and the bispectrum should not be as straightforward as in the radio regime. VLBI algorithms/software should not be well suited to reduce the optical long-baseline data used in the contest. This might arise if visibilitys were missing at times when closure quantities are measured, or vice versa.

The above concerns are noted here for future contests, because this complicated and challenging task was rendered straightforward by necessity. There was no obvious agreement amongst participants as to what should be tested, and only one of the organizers, Christian Hummel, volunteered to create the data. Christian produced sets of data of his own choice, using his data reduction suite OYSTER,* simulating a six-station Navy Prototype Optical Interferometer. The image of the star with asymmetric shell shown in Fig. 1 was provided to Christian by Peter Tuthill. The double star data described in Fig. 2 was simulated within OYSTER. The noise is simulated Poisson noise in 2 ms fringe frames. The errors are not correlated. The simulated measurements were reduced to yield the contest data in exactly the same way that real data would have been processed.

*See the OYSTER website at <http://www.sc.eso.org/~chummel/oyster/oyster.html>

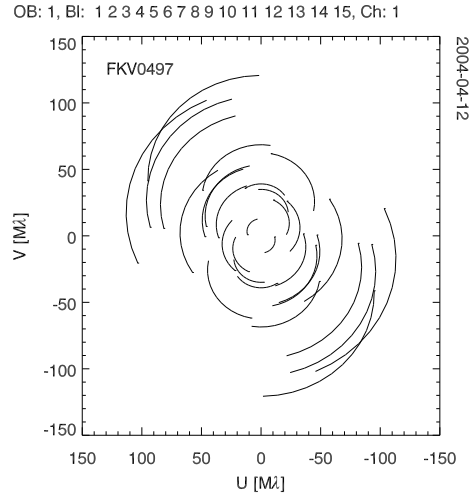
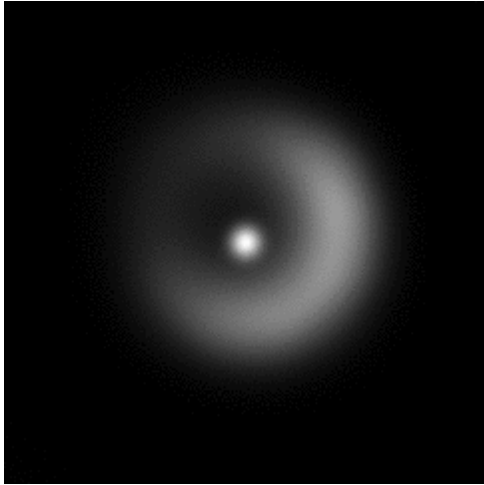


Figure 1. The source file for *Data Set 1* and the u - v plane coverage used to sample the model. A model of LkHa 101, was provided in FITS format by P.G. Tuthill. The 242×242 pixel image was sized with pixels of 0.05 mas on a side and sampled with a simulated six-station Navy Prototype Optical Interferometer (NPOI). About half of the data points are in the low signal-to-noise regime.

```

name(0)          ='A'
mode(0)          =3 ; limb-darkened disk
diameter(0)      =5.5 ; mas
ratio(0)         =0.7 ; minor/major axis
pa(0)           =120.0 ; position angle of major axis east of north
teff(0)         =7000 ; eff. temp. for atmosphere model
logg(0)         =4.0 ; log(g) for atm. mod.
spot(*,0)       =[1.5,2.5,150,1.0]
; bright spot: [=1.5*Teff(star),distance from center (mas),
;              pa east of north, diameter in mas]
;
name(1)          ='B'
mode(1)          =1 ; uniform disk, diam independent of wavelength
diameter(1)      =0.5 ; default is circular
teff(1)         =25000 ; ignore
logg(1)         =5 ; ignore
magnitudes(*,1) =[0.0]
;
; Binary parameters (for each binary):
component(0)     ='A-B'
method(0)        =2
rho(0)          =10.0 ; separation of B from A in mas
theta(0)        =90.0 ; pa east of north

```

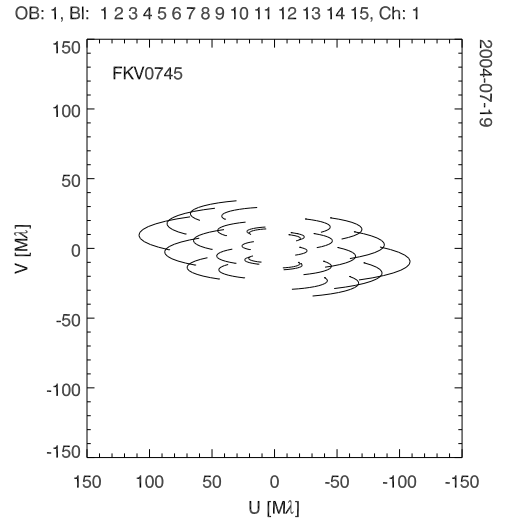


Figure 2. The source file for *Data Set 2* and the u - v plane coverage used to same the model. A double star was simulated within OYSTER. The text on the left is written in the standard model file format for OYSTER. The u - v coverage for a six-station NPOI array is shown on the right. Most of the data points are in the high signal-to-noise regime. Also see the model in Fig. 9.

2.2. Contest Rules and Guidelines

It was agreed amongst the organizers that the contest data sets would only be provided in the OI Exchange Format, hereafter referred to as the OI-FITS format. This obliged contestants to work with this data format before using the data in their programs. Test data were provided as a preliminary to the contest itself. This allowed contestants to see if their software could reproduce a simple image — in this case a binary star with a given separation, magnitude difference, and orientation. The contest data were then presented without any information as to what they represented to provide a blind test. As part of the contest the participants were asked not only to produce images, but to interpret in the images what they believed to be true features and what they believed were artifacts of the imaging process. Deadlines were imposed to provide a consistent schedule compatible with the timetable of the conference.

In the following sections the participants present their results and interpretations. The reader should therefore keep in mind that the images presented in Sections 3 through 6 are the images as submitted to the contest. The conventions for displaying the images (right ascension and declination) and the levels of the contour lines are different in each case. In Section 7 the images are shown again, but this time in a standardized format, all using the same orientation, the same contour lines, and with the same field-of-view. The winning entry is then determined based on a best-fit to reference images.

3. BSMEM

H. THORSTEINSSON AND J. S. YOUNG (UNIVERSITY OF CAMBRIDGE)

3.1. Overview

The software package which we have applied to the contest data sets has been dubbed BSMEM to stand for the BiSpectrum Maximum Entropy Method. This software was first written and completed by Buscher⁴ in 1992 to demonstrate direct maximum entropy⁵ reconstruction from optical aperture synthesis data. BSMEM applies a fully Bayesian approach to the inverse problem of finding the most probable image given the evidence. BSMEM makes use of the MEMSYS library⁶ (Maximum Entropy Data Consultants of Cambridge, UK) to implement a gradient descent algorithm for maximizing the posterior probability of an image. The algorithm has several advantages over its predecessors when applied to optical synthesis data. The phase self-calibration procedure applied more traditionally in interferometry⁷ fails in most cases where the data is mostly composed of the power spectrum with only a very few bispectrum points. Moreover the self-calibration approach relies on the bispectrum and power spectrum components sharing common $u-v$ points. BSMEM's independent treatment of each datum allows it to handle any combination of power spectrum and bispectrum components including any absence of bispectrum-phase or -amplitude. Buscher also notes that one of the method's advantages is its computational cheapness given its reliable treatment of the data. Each of the 256×256 pixel reconstructions which we have obtained from the contest data only took about two minutes of processing on a SUN Ultra workstation to converge.

In the previous two years we have updated the original BSMEM to include the new MEMSYS4 library and added various features to allow for a more interactive way of reconstructing images. We have also developed support software for simulating optical interferometry observations. The present version of the software is written in both Fortran 77 and ANSI C and compiles successfully under Solaris and Linux.

3.2. Procedure

The OI-FITS data sets were successfully read into BSMEM and no information had to be discarded in the image reconstruction. Our general approach involved applying no initial bias towards what the reconstructed images should look like. After an initial reconstruction we would then adjust the pixel size and possibly choose a new default model. The default model is used as a starting model, but it is also treated as a pixel-weighting or bias by MEMSYS. MEMSYS will try to find an image consistent with the data (with χ^2 equal to the number of degrees of freedom) given the user preferences. Using the default model feature we effectively eliminated areas containing artifacts and areas where very little flux is contributed to the image. On restarting the reconstruction we would then observe if the new model improved the regularity of the dominant image components. In the case when our chosen model is not spatially broad enough to allow a good fit to the data the reconstruction will grind to a halt, normally long before $\chi^2 = N$.

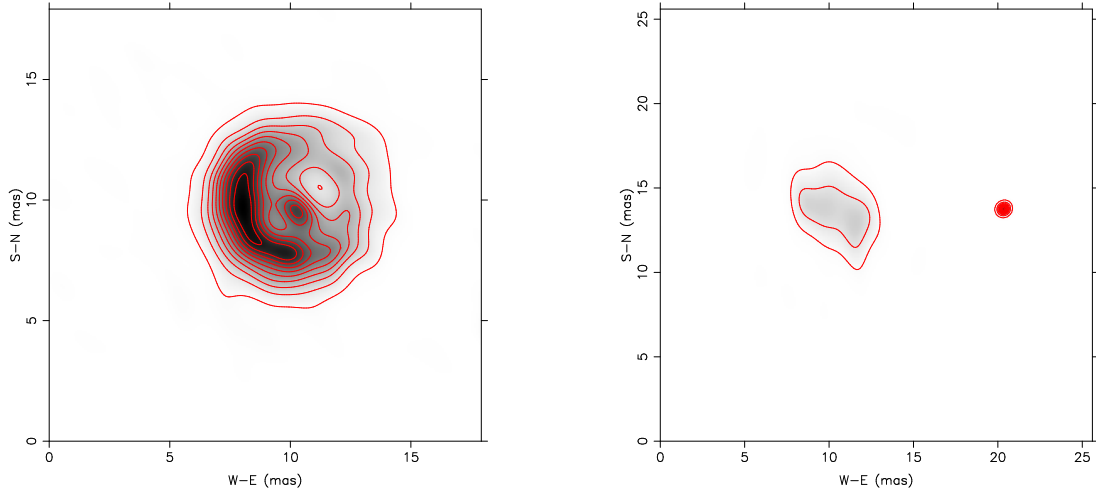


Figure 3. Entries by H. Thorsteinsson and J.S. Young. Results from reconstruction of the contest data sets using BSMEM. The contour levels are at 2, 10, 20, 30, 40, 50, 60, 70, 80, and 90%.

Table 1. BSMEM: Details of image reconstruction

Parameter	<i>Data Set 1</i>	<i>Data Set 2</i>
Data set degrees of freedom	455	455
χ^2 fit to data	302.31	271.91
Number of MEMSYS iterations	71	85
Pixelation (mas/pixel)	0.07	0.10
Map size (pixels)	256×256	256×256

3.3. Results

For *Data Set 1*, after the first reconstructions, we observed that the most reliable image features were located within a 6 or 7 mas diameter disk. Visually the reconstruction shown in Fig. 3 (left) looks somewhere in between a doughnut or a pinwheel in shape. Some amount of prior knowledge about the source would indeed have been helpful in these circumstances and the difference between a stellar disk and an interacting binary system would have significantly affected our choice of default model in this case. We decided to apply a broad Gaussian as a default model to emphasize the central feature in the image but also to allow for some residual flux to extend from the source if BSMEM judged this to be necessary.

For *Data Set 2* we observed a central diffuse feature accompanied by a more compact satellite at about 10 mas to the East. Under the initial even pixel-weighting, the compact feature assumed an elliptical shape with its major axis aligned South-North, the direction of lowest angular resolution. This shape is indeed expected if the object is under-resolved. We therefore decided to constrain the compact feature to be more point-source like and to allow the complex companion to take its shape within a broad Gaussian weighting function. This approach succeeded in making the resolved features more regular in shape and suggested to us that constraining the compact feature to be point-like had successfully constrained the other image components.

4. WISARD

S.C. MEIMON, L. MUGNIER, AND G. LE BESNERAIS (ONERA)

4.1. Overview

WISARD was written to support aperture synthesis imaging with AMBER, the infrared imaging instrument of the Very Large Telescope Interferometer. WISARD was developed at ONERA in collaboration with the Jean-Marie Mariotti Center and follows on from previous work by Laurent Mugnier and Guy Le Besnerais.⁸ It is the subject of Ph.D. research by Serge Meimon.

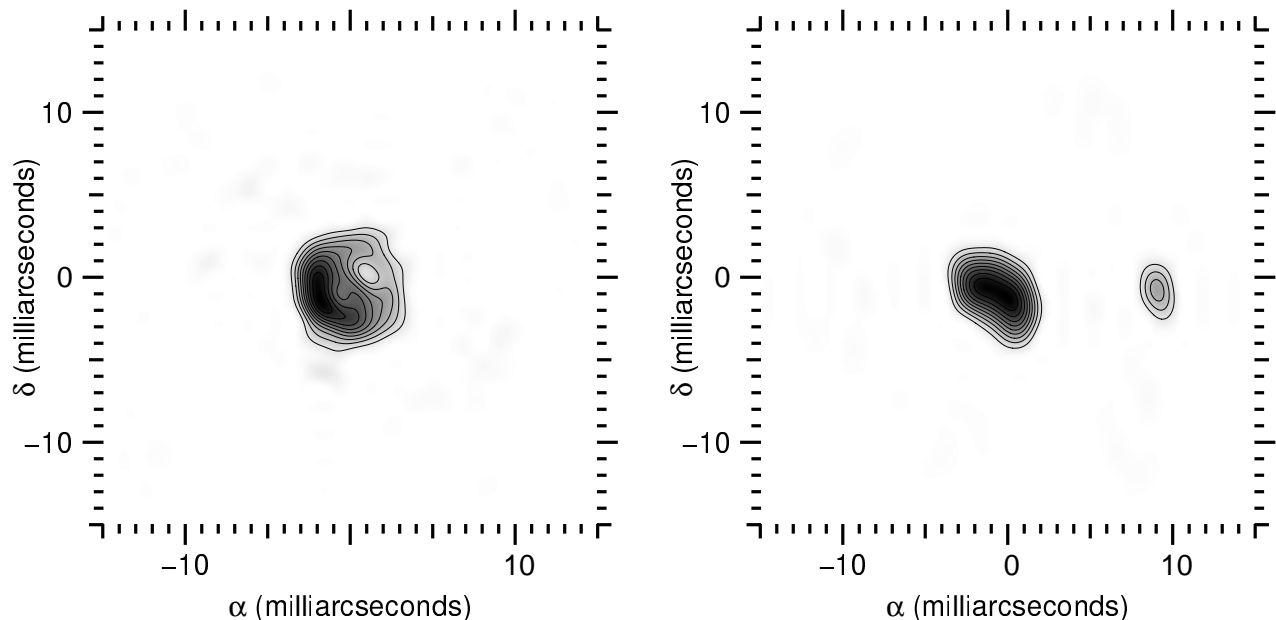


Figure 4. Entries by S.C. Meimon *et al.* Contour levels are at 10, 20, 30, 40, 50, 60, 70, 80, and 90% of the maximum.

We use a Bayesian inversion approach that is faithful to the statistics of the data, while having a well-behaved constrained minimization. The minimization uses VMLM-B⁹ mixed with an exhaustive search step. To handle the lack of direct phase information, we introduce additional explicit variables to be solved in the inversion problem. The resulting criterion includes a regularization term. We get around the lack of phase information by progressively blending the data into the minimizer. The algorithm is implemented in the Interactive Data Language (IDL).

4.2. Procedure

WISARD is designed to deal with optical interferometry data where Fourier phase information is provided only through the closure phases. Currently, WISARD treats any n -element coherent telescope array as a collection of uncorrelated triples, thus it is only optimized for data from three-telescope interferometers. It does not operate as efficiently with data from arrays with four or more telescopes, such as the six-element array data modeled for the contest. However, we are currently working to adapt the algorithm for more general cases. Of the data provided, we used only the squared-visibilitys and closure phases, but not the triple-amplitude data, which were discarded. We initialized the algorithm with a central feature in order to reconstruct an object that was centered in the field. There were no parameters set by the user; WISARD uses only the data statistics and automatically sets the regularization parameters. The minimization stopped when the criterion stabilized. A more detailed description of the algorithm is given elsewhere in these proceedings.¹⁰

4.3. Results

The results we obtained are shown in Fig. 4. The images shown here are interpolated onto a grid of 256×256 pixels. The true outputs of our algorithm, however, are in fact 36×36 pixels for *Data Set 1* and 32×32 pixels for *Data Set 2*. The images, given in the Flexible Image Transport System (FITS) format, have a field of 30×30 mas.

The preliminary phase of the contest, in which data from a test object was reduced, proved very useful to come to grips with the OI-FITS format. It also seemed to us that more information about the size of the object would have been useful as an aid in the reconstruction. However, we look forward to future contests with more challenging data tailored to the strengths of WISARD, with three-telescope configurations and sparser u - v coverage.

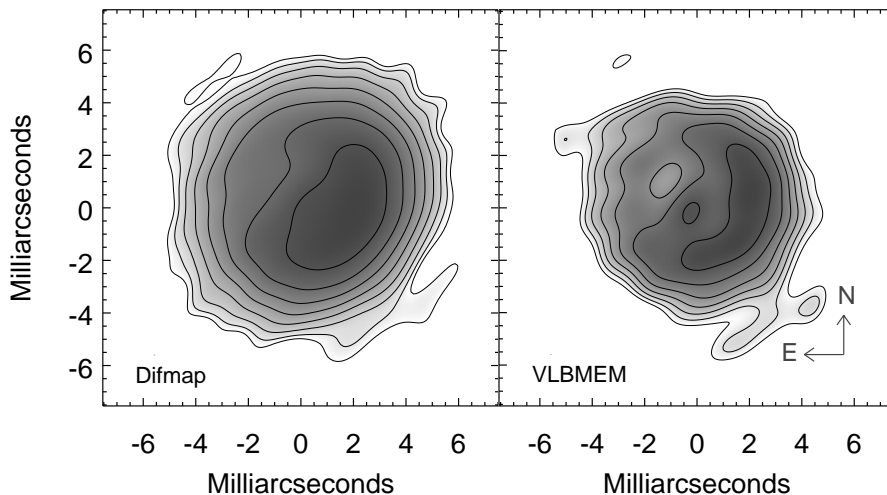


Figure 5. Entries by J.D. Monnier and M. Zhao. Contour levels are at 1, 2, 4, 8, 16, 32, and 64% of the peak. The Difmap image (left) has an additional contour at 0.5%.

5. DIFMAP & VLBMEM

J.D. MONNIER AND M. ZHAO (UNIVERSITY OF MICHIGAN)

5.1. Overview

VLBMEM was developed at the same time and by the same group that performed the first optical aperture synthesis observations. It is a self-contained Fortran implementation of self-calibration which uses the maximum entropy method⁵ for the deconvolution step. It was written by D.S. Sivia at Cambridge University, as part of his Ph.D. thesis¹¹ under the supervision of S.F. Gull. It makes use of MEMSYS, a proprietary software package sold by Maximum Entropy Associates, also used with BSMEM. The program was used for many of the publications by the Cambridge group,^{1, 12–16} and continues to be used for aperture masking work with the Keck-I telescope.¹⁷

Difmap¹⁸ performs the difference mapping algorithm as well as including almost all of the functionality of the Caltech VLBI package¹⁹ incorporated within a single program. Difmap uses a CLEAN²⁰ algorithm as part of the image reconstruction. It is written in ANSI C, and runs on Sun and other UNIX workstations with X-window graphics.

5.2. Procedure and Data Re-formatting

The data sets were supplied in the OI-FITS format and needed to be converted into formats compatible with VLBMEM and Difmap — these programs use only complex visibility information, not closure phases, squared visibilities, or triple amplitudes. This conversion was the most difficult and unpleasant part of the work. Unpleasant because it involved a retrograde step, degrading the quality of the data. The data formats required were (1) MERGE²¹ format for VLBMEM, and (2) UVFITS²² format for Difmap. The data conversion pipeline described below is based on the well-worn track from aperture masking work referred to earlier. The only difficulty lay in creating data in MERGE format. VLBMEM is used routinely to process data from Keck aperture masking experiments, and IDL software already existed to create MERGE files for that task. However, significant enhancements to existing IDL software were required for this project. This included new support for telescope positions, coordinate conversion, array geometry, sidereal motion, Earth-rotation synthesis, and multiple time-stamps.

After reading in the OI-FITS data using a library of IDL routines,²³ an IDL script was written to create a set of complex visibility data consistent with the OI-FITS data products. For each time stamp, a set of phases were generated that were most consistent with the closure phases, using the fix cp algorithm described by Monnier.²⁴ This phase information, along with the visibilities and array information were then written into a MERGE file. A UVFITS file was then created from the MERGE file using the Caltech VLBI program MERGEFITS.

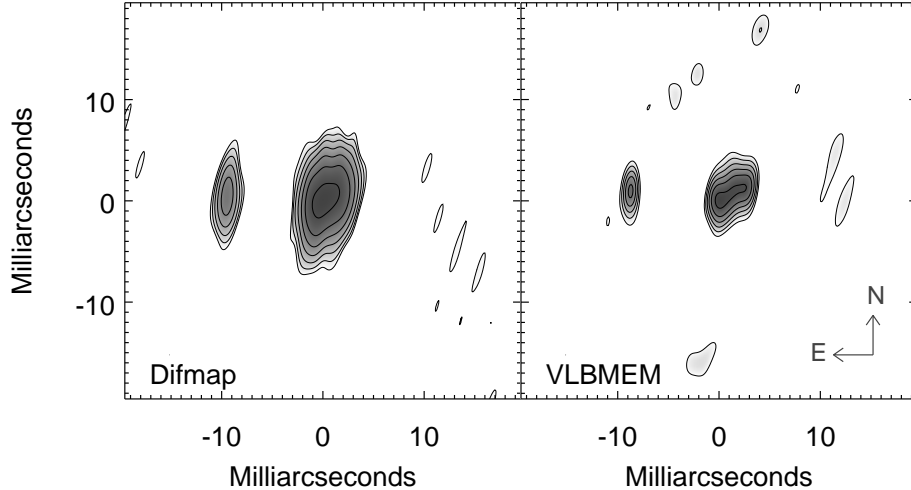


Figure 6. Entries by J.D. Monnier and M. Zhao. Contour levels are at 2.5, 5, 10, 20, 40, and 80% of the peak. The Difmap image (left) has an additional contour at 1.25%.

5.3. Results

Difmap was used to process the UVFITS data. The data were uniformly weighted and the resulting images have 1024 pixels with cell sizes of 0.2 mas. The images were processed following standard CLEAN/self-calibration procedures, suppressing amplitude calibration since closure amplitudes are not good observables in the OI-FITS data files.

VLBMEM was used to process the MERGE data. For *Data Set 1*, a 128×128 pixel map with 0.1 mas pixels was used, employing a 0.4 mas correlation length. There were problems converging for this dataset when using a uniform prior. Good image reconstructions were possible by using Gaussian and Uniform Disk priors which were fit to the raw visibility data; we present only results for Gaussian prior here, but all major image features were present in both. For *Data Set 2*, a 256×256 pixel map with 0.25 mas pixels and 0.4 mas correlation length was used. A uniform prior was used and convergence was not problematic.

We present our results in Fig. 5 and Fig. 6. We chose contour levels such that the lowest-level reveals background artifacts in the maps. Critical image features above the lowest-level contours are present in both methods. The VLBMEM package creates images with higher angular resolution than Difmap, but with a higher level of background artifacts. These artifacts are typically easy to identify but do pose an obstacle for straightforward astrophysical interpretation.

A few features are worth brief mention. The bright spot in the middle of the source shown in Fig. 5 is easily seen in the VLBMEM image (right) but hardly visible in the Difmap image (left) – this feature is at the edge of believability and may represent noise. Note the low-level ring of emission for the VLBMEM image of *Data Set 2*. This is most likely an artifact of the limited Fourier coverage of the observations.

In conclusion, there is good agreement between the two image reconstruction methods. Furthermore, the images show details which appear robust based on their presence in both CLEAN and MEM maps, an impressive result given the limited u - v coverage for the simulated data. Indeed, this is quite remarkable given the data represents merely one night of observing with a realistic six-element interferometer (albeit the data had quite high signal-to-noise ratio). We look forward to imaging real objects in the near future with long-baseline optical interferometry!

We are currently developing image reconstruction algorithms that use OI-FITS data directly, although these algorithms were not sufficiently well advanced to have been included in this contest.

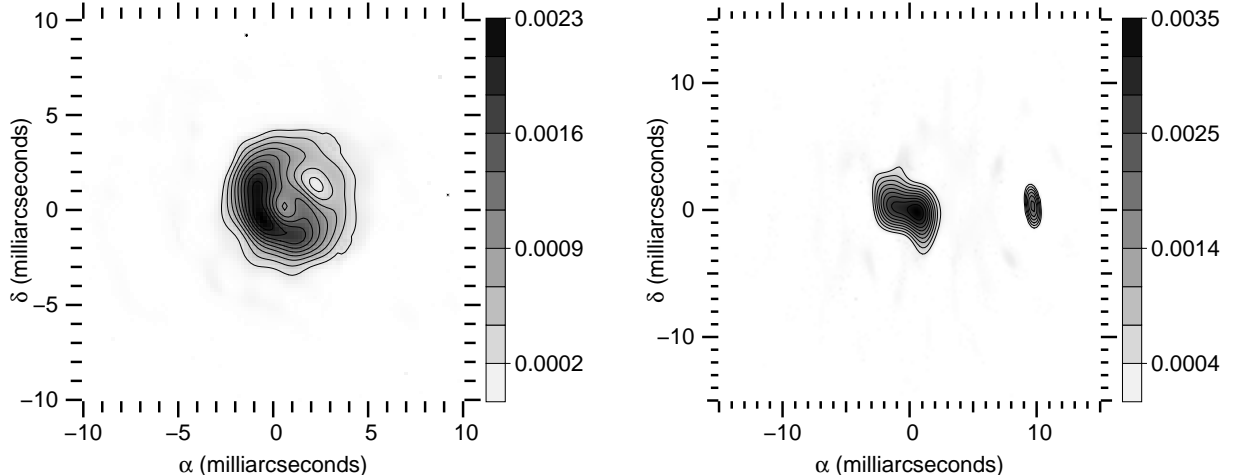


Figure 7. Entries by E. Thiébaud. Contour levels are at 10, 20, 30, 40, 50, 60, 70, 80, and 90% of the maximum.

6. MIRA

E. THIÉBAUD (CRAL / OBSERVATOIRE DE LYON)

6.1. Overview

MIRA (Multi-aperture Image Reconstruction Algorithm) is one of the image reconstruction algorithms being developed at the Jean-Marie Mariotti Center. MIRA is designed to deal with optical interferometry data with sparse u - v coverage and Fourier phase information provided by closure phases.

The principle of the MIRA algorithm is to perform image reconstruction by minimization of a penalty criterion under positivity constraints. The penalty reads:

$$f(\mathbf{x}) = \chi_{\text{vis}^2}^2(\mathbf{x}) + \chi_{\text{cl}}^2(\mathbf{x}) + \mu\mathcal{R}(\mathbf{x}) \quad (1)$$

where \mathbf{x} is a vector representing the parameters (intensity of the image pixels); $\chi_{\text{vis}^2}^2(\mathbf{x})$ is the likelihood term with respect to the visibility-squared data; $\chi_{\text{cl}}^2(\mathbf{x})$ is the likelihood term with respect to the closure phases (defined so as to be insensitive to the modulo- 2π in phase differences); $\mathcal{R}(\mathbf{x})$ is the regularization; μ is a Lagrange multiplier tuned so that at the solution the likelihood terms are equal to their expected values. The constrained minimization is done by VMLM-B.⁹ MIRA is currently written in C and in Yorick (<ftp://ftp-icf.llnl.gov/pub/Yorick/>).

6.2. Procedure and Results

For the contest data, the starting solution of the algorithm was an isotropic Gaussian fitted to the visibility-squared data. This starting solution was also used as the prior for the maximum entropy restorations with a fixed prior. Several different regularizations were considered: (1) Quadratic isotropic smoothness; (2) Maximum entropy with a fixed prior equal to the starting solution (an isotropic two-dimensional Gaussian); (3) Maximum entropy with a floating prior equal to the current solution smoothed to a lower resolution. The use of different types of regularization is an essential aid in determining whether the restored features are real or simply artifacts of imaging — keeping in mind the bias induced by the particular choice of regularization. However, for the two data sets, maximum entropy with a fixed prior seemed to be the method that gave the best results.

The resolution of the restored images was chosen to oversample the data by a factor of roughly two: 0.4 mas per pixel for *Data Set 1* and 0.5 mas per pixel for *Data Set 2*. The regularization levels were tuned (by hand, although plans are underway to automate this process) so that at the solution, the likelihood terms are equal to their expected values. The widths of the synthesized fields of view were chosen to avoid aliasing arising from the space of the sampled frequencies in the u - v plane: 20 and 30 mas for *Data Set 1* and *Data Set 2*, respectively. The results are shown in Fig. 7. The vertical elongation of the secondary component in the image reconstructed from *Data Set 2* is certainly due to the reduced cut-off frequency in that direction (see u - v coverage).

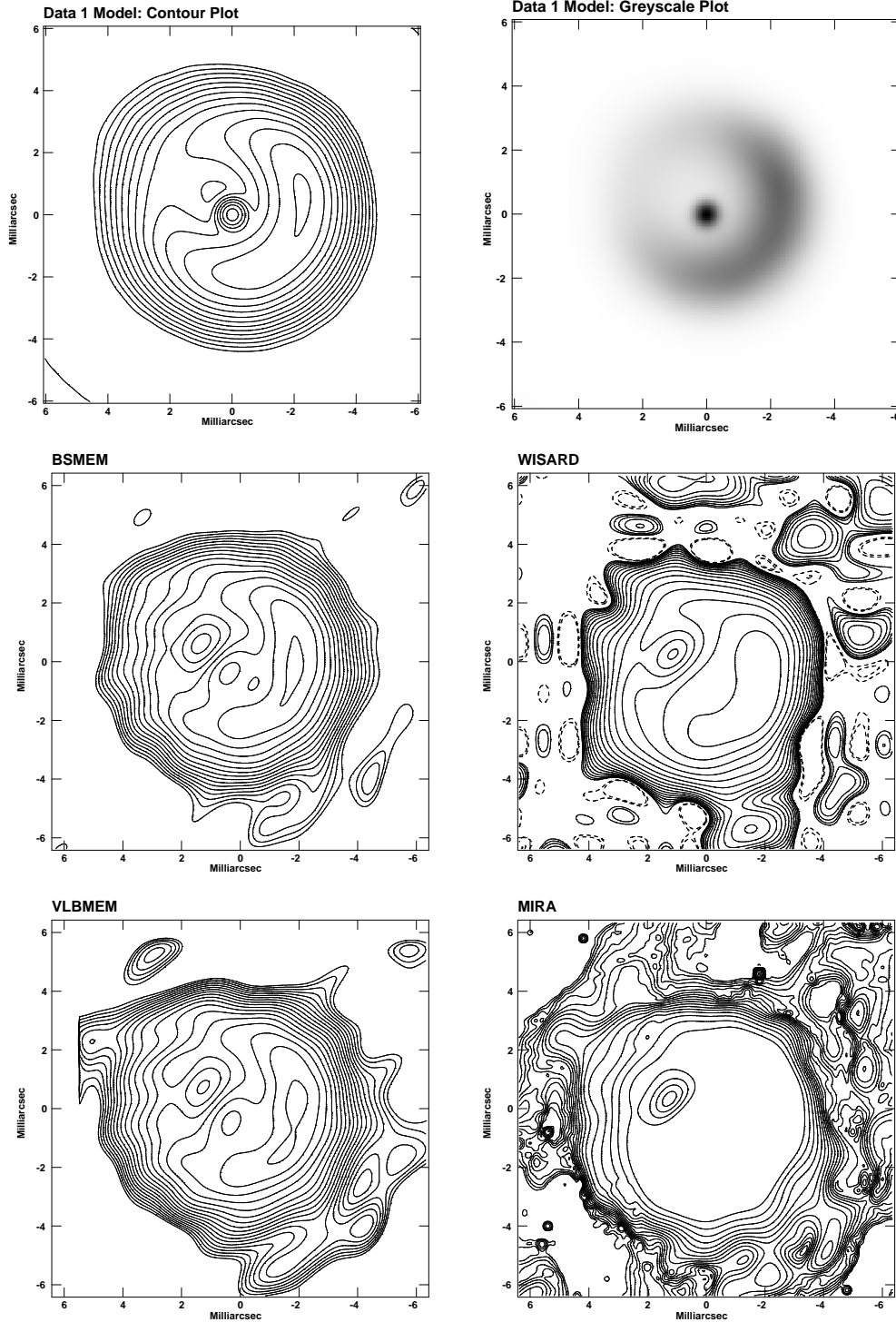


Figure 8. Contest entries for data reduction from *Data Set 1*. The entries have been replotted so that they appear with the same field-of-view and contour levels. Contour levels are multiples of 1.0×10^{-6} , where the factors are -2.00, -1.41, 1.41, 2.00, 2.83, 4.00, 5.66, 8.00, 11.3, 16.0, 22.6, 32.0, 45.3, 64.0, 90.5, 128, 181, 256, 362, and 512. The MIRA image shown here appears saturated compared to the other entries, but when viewed by itself (see Fig. 7) it is obvious that it nonetheless accurately reproduces the surface features.

7. RAPPORT SUR LE CONCOURS DE L'ANNÉE 2004

(COMMISSAIRES: MM. COTTON, HUMMEL, LAWSON RAPPORTEUR.)

The comparison between algorithms was based on calculations derived from FITS images that were submitted as part of the contest. None of the FITS images submitted contained information about the orientation of the source, and for quantitative comparison this information had to be added. Since the algorithms have no information about the position of the source, a fiducial feature in each image was used for alignment. The pixel spacings were explicitly given by the participants and the orientation was determined from the plots shown previously. The comparisons were performed by William Cotton using AIPS.

The images produced by Difmap were not included in the comparisons given here. As can be readily seen, Difmap fared poorly compared with the other imaging algorithms. The contest data simulated measurements of a weakly resolved source, and under these circumstances methods based on the maximum entropy method have an advantage over CLEAN-based algorithms like Difmap. This is particular true when the data have a high signal-to-noise ratio, as was the case here, and maximum entropy is able to plausibly super-resolve the image. CLEAN does an impressively poor job at super-resolution. Without being able to super-resolve the image, Difmap was at a serious disadvantage. Of the entries provided by J.D. Monnier and M. Zhao, only the VLBMEM image was retained for the comparisons.

Table 2. Imaging Beauty Contest Results

	<i>Data Set 1</i>		<i>Data Set 2</i>		$\sum \sigma/\text{peak}$
	σ	σ/peak	σ	σ/peak	
BSMEM	0.000079	0.38	0.00035	0.116	0.50
WISARD	0.00034	1.52	0.00049	0.163	1.68
VLBMEM	0.00024	1.07	0.0024	0.798	1.87
MIRA	0.0012	5.36	0.0016	0.532	5.98

$$\text{Data 1 peak} = 2.239 \times 10^{-4} \quad \text{Data 2 peak} = 3.0677 \times 10^{-1}$$

The comparisons for *Data Set 1* were made with the model image shown in Fig. 1. Similarly, comparisons for *Data Set 2* were made with a model image derived from the parameters shown in Fig. 2. These reference images are shown as contour plots and (negative) greyscale images at the top of Fig. 8 and Fig. 9. The submitted images were labeled and resampled onto the same grid as the reference images. All the displayed plots for a given model (see Fig. 8 and Fig. 9) have the same contour levels. These are multiples of 1.0×10^{-6} for *Data Set 1*, and 5.0×10^{-5} for *Data Set 2*; the multiples are factors of $\sqrt{2}$: Each image was compared with the reference image over a box defined on the reference image containing all the emission. The objective measure was a root-mean-squared agreement, σ , defined as

$$\sigma = \left[\frac{\sum p_{\text{ref}} * (p_i - p_{\text{ref}})^2}{\sum p_{\text{ref}}} \right]^{1/2} \quad (2)$$

where p_i is a pixel in a contest image and p_{ref} is the corresponding pixel in the reference image. The results are shown in Table 2 for each data set. In order to combine the results from the two data sets, the σ s were normalized by the peak brightness in each reference image and then summed. This is possibly not the best way of combining results, although other methods would have been unlikely to change the final outcome. The clear winner by this measure is H. Thorsteinnsson and J.S. Young, the BSMEM entry.

The organizers of the contest, on behalf of the Scientific Organizing Committee of the IAU Working Group on Optical/IR Interferometry, are pleased to announce BSMEM as the winner of the 2004 Interferometry Imaging Beauty Contest. The winning team, Hrobjartur Thorsteinnsson and John Young, were presented with a certificate of their achievement on 25 June 2004 in front of the audience at the SPIE conference on *New Frontiers in Stellar Interferometry* in Glasgow, Scotland.

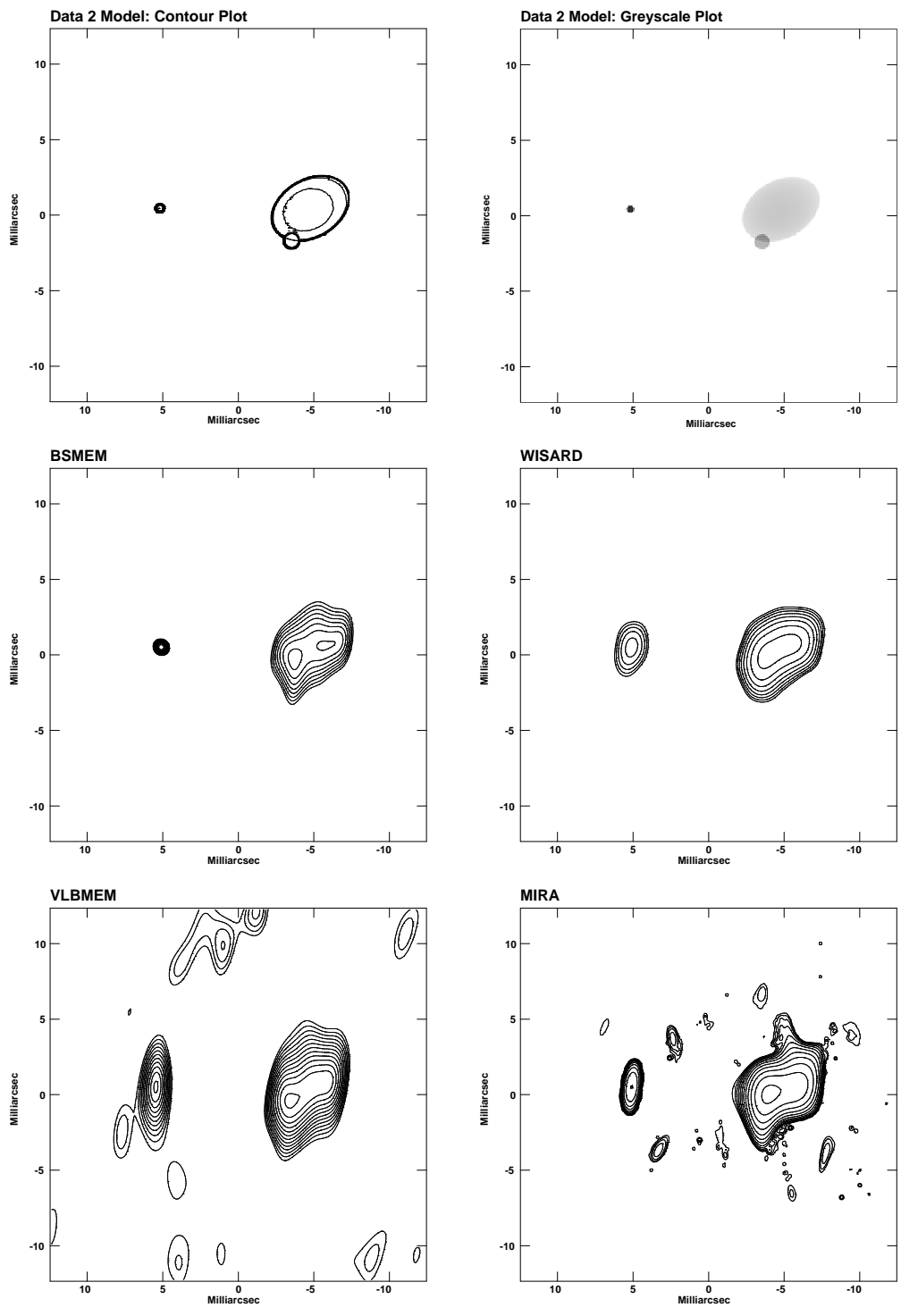


Figure 9. Contest entries for data reduction from *Data Set 2*. The entries have been replotted so that they appear with the same field-of-view and contour levels. Contour levels are multiples of 5.0×10^{-5} , where the factors are -2.00, -1.41, 1.41, 2.00, 2.83, 4.00, 5.66, 8.00, 11.3, 16.0, 22.6, 32.0, 45.3, 64.0, 90.5, 128, 181, 256, 362, and 512.

ACKNOWLEDGMENTS

The organizers had encouraged, but alas ultimately failed to coerce, contributions from Thomas Pauls (Naval Research Laboratory) using AIPS++ and Christopher Haniff (University of Cambridge) using CITVLB. Their efforts and support for the contest are nonetheless sincerely appreciated. It is worthwhile noting that amongst other imaging packages used for interferometry, OYSTER has been one of the most productive. However its author, Christian Hummel, used OYSTER to make the actual contest data and so disqualified himself from the competition. Several source images were initially considered for the contest, including images of exozodiacal dust disks, contributed by Marc Kuchner (Princeton University), and images of jets from a Young Stellar Object, contributed by Paulo Garcia (Universidade do Porto). The organizers are grateful for their help and would furthermore like to acknowledge help and encouragement from Gilles Duvert (Laboratoire d’Astrophysique Observatoire de Grenoble). Work by PRL was carried out at the Jet Propulsion Laboratory, California Institute of Technology, under contract with the National Aeronautics and Space Administration. Work by WDC was supported by the National Radio Astronomy Observatory, a facility of the National Science Foundation operated under cooperative agreement by Associated Universities, Inc. The contest data and further information about the 2004 contest can be found at <http://olbin.jpl.nasa.gov/iau/2004/beauty.html>.

REFERENCES

1. C. A. Haniff, C. D. Mackay, D. J. Titterton, D. Sivia, and J. E. Baldwin, “The first images from optical aperture synthesis,” *Nature* **328**, pp. 694–696, 1987.
2. H. McAlister and T. Cornwell, *Report on the Workshop on Imaging with Ground-based optical interferometers*, National Science Foundation, <http://olbin.jpl.nasa.gov/papers/Report1.0.PDF>, 2000.
3. T. Pauls, J. Young, W. Cotton, and J. Monnier, “A data exchange standard for optical (visible/IR) interferometry,” in *New Frontiers in Stellar Interferometry*, W. Traub, J. Monnier, and M. Schöller, eds., *Proc. SPIE* **5491**, SPIE Press, (Bellingham, WA), 2005.
4. D. Buscher, “Direct maximum-entropy image reconstruction from the bispectrum,” *Proc. IAU Symp.* **158**, pp. 91–93, 1994.
5. S. Gull and J. Skilling, “The maximum entropy method,” in *Indirect Imaging*, J. Roberts, ed., pp. 267–279, Cambridge University Press, (Cambridge, England), 1983.
6. S. Gull and J. Skilling, *Quantified Maximum Entropy, Users Manual*, Maximum Entropy Data Consultants Ltd., 1999. <http://www.maxent.co.uk/>.
7. A. Readhead and P. Wilkinson, “The mapping of compact radio sources from VLBI data,” *Astrophys. J.* **223**, pp. 25–36, 1978.
8. L. Mugnier and G. Le Besnerais, “Problèmes inverses en imagerie optique à travers la turbulence,” in *Approche bayésienne pour les problèmes inverses*, J. Idier, ed., pp. 241–270, Hermès, (Paris), 2001.
9. E. Thiébaud, “Optimization issues in blind deconvolution algorithms,” in *Astronomical Data Analysis II*, J.-L. Starck and F. D. Murtagh, eds., *Proc. SPIE* **4847**, pp. 174–183, SPIE Press, (Bellingham, WA), 2002.
10. S. Meimon, L. Mugnier, and G. Le Besnerais, “A novel method of reconstruction for weak phase optical interferometry,” in *New Frontiers in Stellar Interferometry*, W. Traub, J. Monnier, and M. Schöller, eds., *Proc. SPIE* **5491**, SPIE Press, (Bellingham, WA), 2005.
11. D. Sivia, *Phase Extension Methods*. PhD thesis, University of Cambridge, 1987.
12. D. Buscher, C. Haniff, J. Baldwin, and P. Warner, “Detection of a bright feature on the surface of Betelgeuse,” *Mon. Not. R. Astron. Soc.* **245**, pp. 7p–11p, 1990.
13. R. Wilson, J. Baldwin, D. Buscher, and P. Warner, “High-resolution imaging of Betelgeuse and Mira,” *Mon. Not. R. Astron. Soc.* **257**, pp. 369–376, 1992.
14. P. Tuthill, C. Haniff, J. Baldwin, and M. Feast, “No fundamental-mode pulsation in R Leonis?,” *Mon. Not. R. Astron. Soc.* **266**, pp. 745–751, 1994.
15. P. Tuthill, C. Haniff, and J. Baldwin, “Hotspots on late-type supergiants,” *Mon. Not. R. Astron. Soc.* **285**, pp. 529–539, 1997.
16. P. Tuthill, C. Haniff, and J. Baldwin, “Surface imaging of long-period variable stars,” *Mon. Not. R. Astron. Soc.* **306**, p. 353, 1999.

17. P. G. Tuthill, J. D. Monnier, W. C. Danchi, E. Wishnow, and C. A. Haniff, "Michelson interferometry with the Keck-I telescope," *Pub. Astron. Soc. Pac.* **112**, pp. 555–565, 2000.
18. M. Shepherd, "Difmap: An interactive program for synthesis imaging," in *Astronomical Data Analysis Software and Systems VI*, G. Hunt and H. E. Payne, eds., *ASP Conf. Series* **125**, Astronomical Society of the Pacific, (San Francisco, California), 1997.
19. T. Pearson, *Introduction to the Caltech VLBI Programs*, California Institute of Technology, Pasadena, CA, 1991. <http://www.astro.caltech.edu/~tjp/citvlb/>.
20. B. G. Clark, "An efficient implementation of the algorithm 'CLEAN'," *Astron. Astrophys.* **89**, pp. 377–378, 1980.
21. T. Pearson, "Chapter 11: Format of MERGE files," in *Introduction to the Caltech VLBI Programs*, pp. 11.1–11.4, California Institute of Technology, (Pasadena, CA), 1991. <http://www.astro.caltech.edu/~tjp/citvlb/>.
22. "Chapter 14: FITS tapes," in *Going AIPS: A Programmer's Guide to the NRAO Astronomical Image Processing System*, pp. 14.7–14.10, National Radio Astronomy Observatory, (Charlottesville, VA), 1990. <http://www.aoc.nrao.edu/aips/goaips.html>.
23. J. Monnier, "OI-DATA IDL utilities," in http://www.astro.lsa.umich.edu/~monnier/oi_data/, (University of Michigan), 2004.
24. J. D. Monnier, *Infrared Interferometry and Spectroscopy of Circumstellar Envelopes*. PhD thesis, University of California at Berkeley, Dec. 1999.